Optics Letters

Arithmetic with optical topological charges in stepwise-excited Rb vapor

Alexander M. Akulshin,[1,*] Irina Novikova,[2] Eugeniy E. Mikhailov,[2] Sergey A. Suslov,[3] and Russell J. McLean[1]

[1]Centre for Quantum and Optical Science, Swinburne University of Technology, Melbourne, Australia
[2]College of William & Mary, Williamsburg, Virginia 23185, USA
[3]Department of Mathematics, Faculty of Science, Engineering and Technology, Swinburne University of Technology, Melbourne, Australia
*Corresponding author: aakoulchine@gmail.com

Received 24 December 2015; revised 1 February 2016; accepted 3 February 2016; posted 3 February 2016 (Doc. ID 256424); published 8 March 2016

We report on experimentally observed addition, subtraction, and cancellation of orbital angular momentum (OAM) in the process of parametric four-wave mixing that results in frequency up- and down-converted emission in Rb vapor. Specific features of OAM transfer from resonant laser fields with different optical topological charges to the spatially and temporally coherent blue light (CBL) have been considered. We have observed the conservation of OAM in nonlinear wave mixing in a wide range of experimental conditions, including a noncollinear geometry of the applied laser beams, and furthermore, that the CBL accumulates the total OAM of the applied laser light. Spectral and power dependences of vortex and plane wavefront blue light beams have been compared.

OCIS codes: (190.4223) Nonlinear wave mixing; (190.4975) Parametric processes; (020.1670) Coherent optical effects.

http://dx.doi.org/10.1364/OL.41.001146

Structured light [1,2] is a rapidly emerging subfield of optics. Optical vortices are of great interest, owing to their numerous prospective applications, including optical communication [3], particle manipulation [4], and quantum information processing [5].

Vortex, or twisted, light is characterized by a helical phase front. A vortex beam usually has an annular ring intensity profile with a phase singularity at the beam center, which results in vanishing on-axis light intensity. Analytically, a vortex beam could be characterized based on paraxial eigensolutions of the wave equation in cylindrical coordinates, i.e., the Laguerre–Gaussian (LG) modes. Every photon of vortex light carries $|\ell|\hbar$ orbital angular momentum (OAM), where integer ℓ called the optical topological charge is equal to the number of twists in a wavefront per unit wavelength. Positive and negative values of ℓ correspond to clockwise and counterclockwise rotation of the wave vector around the beam axis, respectively, while $\ell = 0$ describes a beam with a plane phase.

Much attention has been also given to the study of soliton-type vortex light propagation in nonlinear bulk and atomic media [6]. One of the first demonstrations of OAM transfer from the applied laser light to a generated optical field of similar wavelength was realized via parametric wave mixing in cold Cs atoms [7]. Later, it was proven that the optical topological charge ℓ is conserved during a nonlinear process. The conservation and entanglement of OAM in a parametric frequency down-conversion process was demonstrated in [5], and the storage of OAM of light and its subsequent retrieval has been achieved in warm atomic vapors [8] and in an ensemble of cold atoms [9]. Recently, conservation of OAM in degenerate four-, six- and eight-wave mixing was reported in a laser-cooled atomic sample [10]. The transfer of OAM from laser light to optical fields from different spectral regions generated in atomic media due to parametric four-wave mixing (FWM) was also reported [11–13]. Optical topological charge conservation was used to distinguish nonlinear processes in atomic media [13].

Here we report experimental observations of optical topological charge transfer from the applied laser radiation to spatially and temporally coherent blue light (CBL) generated in Rb vapor as a result of a parametric FWM process [14–16]. The topological charge of the frequency up-converted light is related to the applied laser light charges via simple arithmetical operations, such as addition and subtraction. Better understanding of the OAM transfer from laser light to frequency-converted radiation is particularly important for preparing entangled light fields from different spectral regions.

The coherent blue and mid-IR light generation occurs in atomic Rb vapor stepwise-excited to the $5D_{5/2}$ level, as illustrated in Fig. 1(a). A schematic of our experimental setup depicted in Fig. 1(b) is similar to that previously described in [13,16].

The resonant radiation at 780 and 776 nm is provided by two extended cavity diode lasers. Typically, the angle between the two laser beams does not exceed 0.5 mrad, although in some experiments the laser beams are crossed inside the cell at larger angles, up to 14 mrad. The combined bichromatic

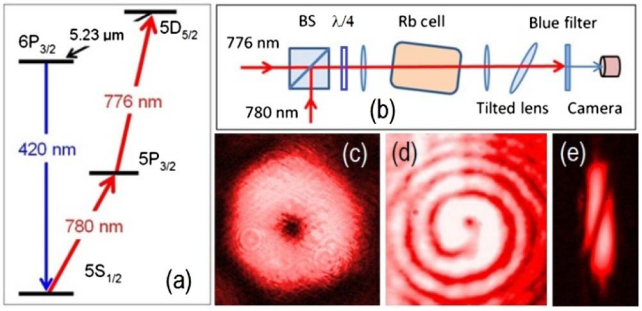

Fig. 1. (a) Schematic of Rb atom energy levels involved in stepwise excitation and subsequent FWM process; (b) sketch of the experimental setup; (c) intensity cross section of single-charged vortex laser light ($\ell = +1$) taken by CCD; (d) single-arm spiral interference pattern of single-charged vortex and plane wavefront laser beams; (e) tilted lens profile of single-charged vortex laser light.

laser beam is sent through a polarizer, a quarter-wave plate and a Rb vapor cell. In this work we use a heated 5-cm long glass cylindrical cell containing Rb vapor with natural isotopic abundance and without buffer gas. The maximum laser powers at 780 and 776 nm before entering the cell are 10 and 5 mW, respectively. In most cases, the circularly polarized applied laser light is gently focussed to a waist of ~100 μm inside the cell. The cell axis is intentionally tilted with respect to the direction of the combined laser beam by approximately 100 mrad to minimize a cell orientation effect, which will be discussed elsewhere.

The Rb atom number density evaluated by using recorded absorption profiles on the Rb D2 line and specialized software [17] is kept within the range of $(0.05 - 2) \times 10^{12}$ cm^{-3}, where collisional broadening is negligible [18].

The optical frequency of the first-step laser at 780 nm is either locked to a Doppler-free dispersion-shaped polarization resonance obtained in an auxiliary Rb cell on the ^{85}Rb $5S_{1/2}$ $(F = 3) - 5P_{3/2}(F' = 4)$ transition, or scanned across the Doppler-broadened absorption profile on the $5S_{1/2}(F = 3) - 5P_{3/2}$ transition. The frequency of the second-step laser at 776 nm is tuned to maximize the CBL power.

Vortex laser light is created using a phase mask or a blazed diffraction grating with a fork-type singularity. The phase mask for single-charged vortex generation is an optical spiral staircase structure with eight radial sectors that progressively build the total phase difference of 2π after a complete rotation of the azimuthal angle.

Figure 1(c) shows the intensity profile of laser light transmitted through the phase mask. The zero intensity at the beam core suggests a phase singularity. However, a doughnut-type intensity profile is a necessary, but not sufficient, condition for an optical beam to be vortex-bearing. Observing a spiral-shaped interference pattern produced by mixing with a plane wavefront reference beam [Fig. 1(d)] is the most convincing way to demonstrate the nonzero topological charge of an optical beam. However, in the case of CBL, this technique is not straightforward, as reference blue light produced independently, even by the same lasers, might have slightly different optical frequencies [19], preventing the observation of a stationary interference pattern.

Several methods exist for measuring the optical topological charge or OAM quantum number [1,2], but we find that in our case the tilted convex lens method [20], which relies on the astigmatic transformation of an optical vortex beam in the vicinity of the focal plane [21], is the most suitable approach because of its simplicity and robustness. The number of high-contrast dark stripes across the vortex beam image produced by a tilted lens is equal to the topological charge carrying by the beam, as Fig. 1(e) illustrates.

First, we consider the situation when FWM occurs with one twisted and one plane phase-front laser beam. Typical images of CBL produced by a single-twisted 776 nm and plane phase-front 780 nm laser beam are shown in Fig. 2. In the case of perfectly overlapping laser beams, the experimentally observed CBL doughnut-shaped intensity cross section [Fig. 2(a)] looks similar to the LG_0^1 mode. The topological charge of the CBL is revealed by its transformed image, obtained with a tilted lens [Fig. 2(b)]. This image is very similar to the result shown in Fig. 2(c) of our numerical modeling, which follows the methodology of Ref. [20], of the intensity profile of a single-charged vortex beam in the vicinity of the focal plane of the tilted lens. A single high-contrast dark stripe appearing across the image indicates that the CBL beam carries a single topological charge. This means that the single unit of OAM has been transferred from the laser light at 776 nm to the blue light in the FWM process. If the first-step laser light at 780 nm carries a single topological charge instead of the 776 nm laser light, OAM also transfers to the CBL.

We have repeated this experiment over a wide range $(0.05 - 2) \times 10^{12}$ cm^{-3} of Rb number densities, as well as under more than 50-fold laser intensity variations and with linearly polarized laser light. We find that the transverse intensity profile of the generated CBL is a complex function of alignment, laser frequency detuning, polarizations and intensities of the applied laser fields, as well as the atom number density N, and the magnetic field environment. Nevertheless, the high-contrast dark stripes across the tilted lens CBL images are always present, confirming that the blue light accumulates the total topological charge of the laser light.

The transfer of OAM from laser light to CBL occurs even if the applied laser beams are not perfectly collinear. In this case, the direction of vortex CBL determined by the phase-matching condition ($k_1 + k_2 = k_{IR} + k_{BL}$, where k_1, k_2, k_{IR}, and k_{BL} are the wave vectors of the light beams at 780 nm, 776 nm, 5.23 μm, and 420 nm, respectively) does not coincide with the direction of either of the laser beams.

Figure 3(a) shows intensity profiles of the applied laser beams at 780 and 776 nm that intersect inside the Rb cell at 6 mrad. The CBL images in Figs. 3(b) and 3(c) are

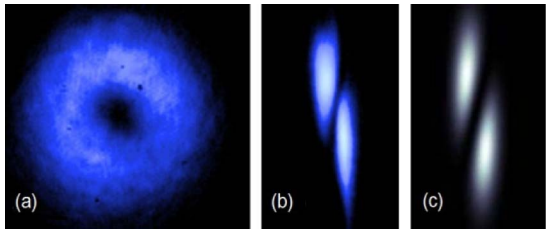

Fig. 2. Intensity profiles of CBL produced with single-charged vortex light at 776 nm ($\ell = +1$) and plane wavefront light at 780 nm ($\ell = 0$) (a) without and (b) with lens tilting, respectively, at Rb atom number density $N \approx 0.5 \times 10^{12}$ cm^{-3}; (c) calculated tilted lens profile of single-charged vortex light $\ell = +1$.

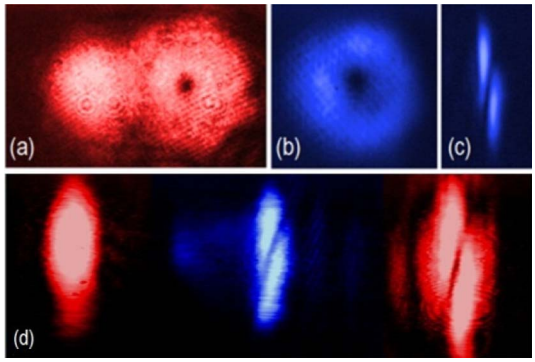

Fig. 3. (a) Intensity profiles of the applied single-charged vortex laser light at 776 nm and plane wavefront light at 780 nm crossed inside the Rb cell with $N \approx 3.5 \times 10^{11}$ cm^{-3}. The laser beam intersection angle inside the cell is 6 mrad; (b),(c) intensity profiles of blue light generated by noncollinear laser beams without and with lens tilting, respectively; (d) simultaneous detection of plane wavefront light at 780 nm (left), vortex light at 776 nm (right) and the resulting blue vortex light produced with applied fields crossed inside the Rb cell at the 14 mrad maximum angle imposed by the cell heater design.

remarkably similar to the images obtained for the collinear geometry discussed above. The high-contrast dark stripe convincingly demonstrates that the $\ell = +1$ topological charge has been transferred to CBL, despite the angle between the laser beams.

OAM transfer occurs even at larger crossing angles. Figure 3(d) shows well-separated tilted lens images of both laser beams and CBL detected simultaneously. The characteristic high-contrast tilted dark stripes confirm the transfer of a single topological charge to the CBL.

A violation of the total OAM conservation in the case of FWM of noncollinear vortex beams in a bulk medium was recently reported [22]. Although such violation, to our knowledge, has not been observed in atomic media, the peculiarities of OAM transfer from the noncollinear vortex laser light to the product of parametric FWM require further examination. Of particular interest is the transition to conical emission that is common for parametric FWM [23], as well as an evaluation of the critical angle for the OAM conservation and other restrictions imposed by the applied laser light geometry.

In the previous experiment on OAM transfer to blue light [12], a single spatial light modulator was used for applying the same topological charge simultaneously to both laser fields. In our study, independently prepared vortex light at 776 and 780 nm provides new opportunities for analyzing the details of the optical topological charge transfer.

We first produce a single-charged vortex beam at 780 nm using the forked grating ($\ell_{780} = +1$), combine this beam with the plane phase-front light at 776 nm ($\ell_{776} = 0$), then send the combined bichromatic output through the single-charge phase mask, and finally compare the topological charges of CBL generated in the case of two opposite orientations of the mask.

In one orientation, the phase mask adds one unit of a topological charge ($\ell = +1$) to both the transmitted laser fields, making the 776 and 780 nm laser light single- and double-charged, respectively. Thus, the applied laser light carries three units of OAM, since $\ell = \ell_{780} + \ell_{776} = 3$. Three clearly

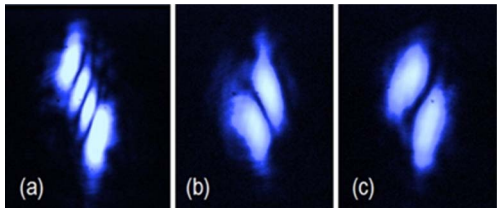

Fig. 4 (a)–(c). Images of CBL with different total topological charges ($\ell_{CBL} = +3, \ell_{CBL} = -1$, and $\ell_{CBL} = +1$, respectively) observed using the tilted lens method.

resolved dark strips across the tilted lens image [Fig. 4(a)] demonstrate that this total OAM has been accumulated by blue light.

The oppositely oriented phase mask in the combined beam adds one unit of negative topological charge ($\ell = -1$) to both laser fields, producing OAM compensation for the 780 nm laser light ($\ell_{780} = 0$) and single-charged vortex at 776 nm ($\ell_{776} = -1$). Such laser light generates vortex CBL with the opposite chirality or negative topological charge ($\ell_{CBL} = -1$), as evidenced by the single dark stripe with the opposite inclination across the image show in Fig. 4(b). No phase mask in the combined bichromatic beam results in CBL with single positive topological charge ($\ell_{CBL} = \ell_{780} = +1$), as Fig. 4(c) demonstrates. The observed accumulation on total OAM of the applied laser radiation by the frequency up-converted light was attributed in [18] to the spatial overlap with the laser fields being better for the CBL than for 5.23 μm light.

We also find that the applied vortex laser light can produce OAM-free CBL if the equally charged vortices at 780 and 776 nm have opposite-handedness. The observed cross section of the intensity of blue light generated by the single-charged vortex laser light at 780 and 776 nm with opposite chirality is shown in Fig. 5(a). Here the doughnut-type intensity profile of the CBL results from the zero on-axis intensity in both applied laser beams. The tilted lens image in Fig. 5(b) does not contain a characteristic dark stripe. Instead, it closely resembles the calculated image of a vortex-free beam with a doughnut-type intensity distribution [Fig. 5(c)]. That confirms that such pseudovortex light does not carry any topological charge, despite its doughnut-type intensity profile. Figure 5(d) demonstrates the tilted lens image of CBL generated under exactly the same experimental conditions, but with the same handedness of single-charged vortex laser light at 776 and 780 nm ($\ell_{780} = \ell_{776} = +1$). Two high-contrast dark stripes across the tilted

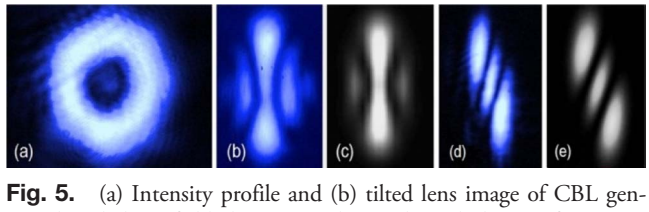

Fig. 5. (a) Intensity profile and (b) tilted lens image of CBL generated with laser fields having single topological charge of opposite helicity ($\ell_{780} = +1$ and $\ell_{776} = -1$); (c) calculated tilted lens image of vortex-free beam with doughnut-shaped intensity cross section (pseudovortex light); (d) tilted lens profile of CBL generated with the same handedness of single-charged vortex laser light at 776 and 780 nm ($\ell_{780} = \ell_{776} = +1$); (e) calculated tilted lens profile of double-charged vortex light.

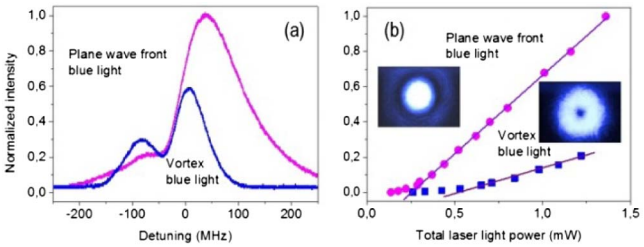

Fig. 6. (a) Intensity of plane wavefront and double-charged vortex blue light as a function of frequency detuning of the 780 nm laser from the ^{85}Rb $5S_{1/2}(F = 3) - 5P_{3/2}(F' = 4)$ transition, while the frequency of the 776 nm laser is tuned to the peak vortex blue light intensity for zero detuning of the 780 nm laser; (b) power dependence of plane wavefront and double-charged blue light.

lens image indicate that in this case the frequency up-converted light carries two units of OAM, accumulating the total topological charge of the applied laser light. The calculated tilted lens profile of a double-charged vortex beam [Fig. 5(e)] is consistent with the experimentally observed image.

Finally, we compare power and spectral characteristics of the vortex and vortex-free CBL. To eliminate effects attributed to different spatial characteristics of the applied laser beams at 780 and 776 nm (e.g., different divergence, astigmatism, diameter, and their mutual overlapping), the combined beam is first transmitted through a single-mode fiber, making spatial properties of the laser fields at 780 and 776 nm identical.

Figure 6(a) shows typical dependences on the 780 nm laser frequency detuning of plane phase-front and vortex CBL generated in the Rb cell under the same experimental conditions. The spectral dependences are significantly different in amplitude and width. It appears that the vortex CBL is generated over a significantly narrower range of 780 nm laser frequencies than for plane phase-front light. We also find that vortex CBL has a higher threshold and its power grows more slowly compared to the plane wavefront blue light [Fig. 6(b)].

We attribute these effects of intensity reduction and spectral profile narrowing to less efficient excitation of the Rb atoms. Indeed, the peak intensity of the vortex laser light is significantly lower than that of the plane wavefront light because of increased cross section and approximately 5% intensity reduction due to transmission through the phase mask. This could be also due to the fact that the pencil-shaped excitation region formed by vortex laser light inside the Rb cell contains no excited atoms along the longitudinal axis, making the process of ASE less efficient, leading to a higher threshold for 5.23 μm field, and its lower intensity in turn increases the threshold and reduces the intensity of the CBL.

We also note that the optimal frequency tuning of the applied laser fields is different for vortex and plane wavefront CBLs. Detailed analysis of spectral and intensity properties of CBL will be the subject of a separate paper.

In summary, the transfer of optical topological charge from resonant laser light to temporally and spatially coherent frequency up-converted emission generated in stepwise-excited Rb vapors has been experimentally investigated. The topological charge of the generated collimated blue light has been measured by the tilted lens method. The ability of this method to distinguish between real and pseudo-optical vortex beams having similar doughnut-like intensity profiles has been confirmed by our numerical modeling and experimental observations.

It has been found that the CBL produced by parametric FWM accumulates the total OAM of the applied laser light for a wide range of experimental parameters, such as 50-fold variations of the applied laser power, Rb number density variations in the range $(0.05 - 2) \times 10^{12}$ cm^{-3}, and noncollinear geometry of the applied laser beams. An important avenue for further work would be to investigate the transfer in more symmetric diamond-type systems.

Spectral and power dependences of vortex and plane phase-front blue light reveal that the vortex laser light generates less intense CBL over a narrower spectral range compared to plane phase-front light. We explain this fact by less efficient stepwise excitation of Rb atoms and weaker amplified spontaneous emission in the region along the longitudinal axis with no excited atoms.

Acknowledgments. We thank A. Sidorov for useful discussions, B. Hall for the use of his laser system, and Grover Swartzlander for the loaning of the vortex phase mask.

REFERENCES

1. M. S. Soskin and M. V. Vasnetsov, Prog. Opt. **42**, 219 (2001).
2. A. Yao and M. Padgett, Adv. Opt. Photon. **3**, 161 (2011).
3. G. Gibson, J. Courtial, M. J. Padgett, M. Vasnetsov, V. Pasko, S. M. Barnett, and S. Franke-Arnold, Opt. Express **12**, 5448 (2004).
4. M. Padgett and R. Bowman, Nat. Photonics **5**, 343 (2011).
5. A. Mair, A. Vasiri, G. Weihs, and A. Zeilinger, Nature **412**, 313 (2001).
6. A. Desyatnikov, Y. Kivshar, and L. Torner, Prog. Opt. **47**, 291 (2005).
7. J. W. R. Tabosa and D. V. Petrov, Phys. Rev. Lett. **83**, 4967 (1999).
8. R. Pugatch, M. Shuker, O. Firstenberg, A. Ron, and N. Davidson, Phys. Rev. Lett. **98**, 203601 (2007).
9. D. Moretti, D. Felinto, and J. Tabosa, Phys. Rev. A **79**, 023825 (2009).
10. R. A. de Oliveira, G. C. Borba, W. S. Martins, S. Barreiro, D. Felinto, and J. W. R. Tabosa, Opt. Lett. **40**, 4939 (2015).
11. D.-S. Ding, Z.-Y. Zhou, B.-S. Shi, X.-B. Zou, and G.-C. Guo, Opt. Lett. **37**, 3270 (2012).
12. G. Walker, A. S. Arnold, and S. Franke-Arnold, Phys. Rev. Lett. **108**, 243601 (2012).
13. A. M. Akulshin, R. J. McLean, E. E. Mikhailov, and I. Novikova, Opt. Lett. **40**, 1109 (2015).
14. A. S. Zibrov, M. D. Lukin, L. Hollberg, and M. O. Scully, Phys. Rev. A **65**, 051801 (2002).
15. J. F. Sell, M. A. Gearba, B. D. DePaola, and R. J. Knize, Opt. Lett. **39**, 528 (2014).
16. A. Akulshin, D. Budker, and R. McLean, Opt. Lett. **39**, 845 (2014).
17. Rochester Scientific, http://rochesterscientific.com/ADM.
18. A. M. Akulshin, A. A. Celikov, V. A. Sautenkov, T. A. Vartanian, and V. L. Velichansky, Opt. Commun. **85**, 21 (1991).
19. A. M. Akulshin, C. Perrella, G.-W. Truong, R. J. McLean, and A. Luiten, J. Phys. B **45**, 245503 (2012).
20. P. Vaity, J. Banerji, and R. P. Singh, Phys. Lett. A **377**, 1154 (2013).
21. A. Y. Bekshaev, M. S. Soskin, and M. V. Vasnetsov, Opt. Commun. **241**, 237 (2004).
22. T. Roger, J. J. F. Heitz, E. M. Wright, and D. Faccio, Sci. Rep. **3**, 3491 (2013).
23. W. Chalupczak, W. Gawlik, and J. Zachorowski, Opt. Commun. **99**, 49 (1993).